

The onset of secondary phase precipitation during synthesis of heteroepitaxial $\text{Si}_{1-x-y}\text{Ge}_x\text{C}_y$ on Si(100)

Nicole Herbots, Peihua Ye, Harald Jacobsson, Joan Xiang, and Sean Hearne
Department of Physics & Astronomy, Arizona State University, Tempe, Arizona 85287-1504

Nigel Cave

Materials Research and Strategic Technologies, Motorola Inc., Mesa, Arizona 85213

(Received 11 July 1995; accepted for publication 28 November 1995)

An upper temperature limit of 450 °C has been established for growth of heteroepitaxial $\text{Si}_{1-x-y}\text{Ge}_x\text{C}_y$ solid solutions with substitutional C on Si(100) by combined ion and molecular beam deposition (CIMD). At 450 °C infrared absorption spectroscopy shows that C is on substitutional sites and no SiC precipitates are detected, whereas at 560 °C the substitutional C signal is much smaller but SiC precipitates are still not detected. High resolution transmission electron microscopy shows that $\text{Si}_{1-x-y}\text{Ge}_x\text{C}_y$ films deposited at 560 °C exhibit Ge deficient, coherent, secondary phase clusters in the cubic diamond matrix, which are not seen in films deposited at 450 °C. These observations suggest that the clusters are C-rich, Ge-deficient precursors to SiC, with a lattice which is distorted but free of extended defects. Ion channeling results indicate that the $\text{Si}_{1-x-y}\text{Ge}_x\text{C}_y$ films might have a distribution of different bond lengths. © 1996 American Institute of Physics. [S0003-6951(96)00305-9]

Significant material development in group IV-IV semiconductors has occurred lately: both bipolar and field effect device technology and bandgap modulation can now be achieved by heteroepitaxy of $\text{Si}_{1-x}\text{Ge}_x$ alloys on Si using far-from-equilibrium deposition methods.^{1,2} However, the maximum bandgap offset in $\text{Si}_{1-x}\text{Ge}_x$ alloys on Si is limited to 0.4 eV and strain engineering is limited by the Ge atomic fraction. Therefore, heteroepitaxy of ternary $\text{Si}_{1-x-y}\text{Ge}_x\text{C}_y$ alloys on Si has recently become the object of intense scrutiny. Adding C to $\text{Si}_{1-x}\text{Ge}_x$ may expand the accessible range of bandgap offsets and provide a new degree of freedom for lattice matching on Si(100).^{3,4}

In contrast to $\text{Si}_{1-x}\text{Ge}_x$ binary alloys, where Si and Ge are entirely miscible into each other, the solid solubility of C in bulk Si is limited to 10^{18} atoms/cm³ for $T \leq 1400$ K.⁵ Beyond that limit, SiC polytype phases precipitate. Carbon is immiscible in bulk Ge.⁶ In thin film phases, far-from-equilibrium synthesis can kinetically control phase separation in a solid solution, such as $\text{Si}_{1-x-y}\text{Ge}_x\text{C}_y$. In previous studies, the formation of heteroepitaxial $\text{Si}_{1-x-y}\text{Ge}_x\text{C}_y$ solid solutions $x \leq 0.2$, $y \leq 0.02$ has been demonstrated by molecular beam epitaxy (MBE)⁴ as well as by ion implantation and subsequent solid phase epitaxial regrowth.⁷

The temperature of formation of SiC precipitates in Si with C impurity concentrations $\leq 10^{18}$ cm⁻³ is fairly high: 800 °C at Si surfaces,⁸ and 1000–1250 °C in bulk Si.⁹ However, during annealing of $\text{Si}_{1-y}\text{C}_y$ with C concentrations $\geq 10^{20}$ cm⁻³, loss of substitutional C is significant already at 810 °C, but SiC precipitates are not formed until most of the C is lost from substitutional sites.¹⁰ During growth of $\text{Si}_{1-y}\text{C}_y$ no SiC precipitation was reported at temperatures in the range 450 to 750 °C, but a maximum in the substitutional C signal was observed in the Raman spectra at a growth temperature of 525 °C.¹¹ The temperature dependence of C incorporation in $\text{Si}_{1-x-y}\text{Ge}_x\text{C}_y$ has not been reported. While Ge alloying makes Si less refractory, C alloying is expected to have the opposite effect. Hence an accurate thermody-

namical prediction is difficult to make, which led to the present work investigating the temperature threshold for carbide precipitation in $\text{Si}_{1-x-y}\text{Ge}_x\text{C}_y$.

Heteroepitaxial $\text{Si}_{1-x-y}\text{Ge}_x\text{C}_y$ thin films are synthesized on 4 in. Si(100) wafers in a combined ion and molecular beam deposition (CIMD)¹² system. Molecular Si and Ge are evaporated from conventional e-beam sources. A partially ionized (~40%), C⁺ beam is obtained from a solid 99.9995% pyrolytic graphite source. Direct deposition of the ionized C during CIMD, can limit the surface mobility of C by “anchoring” the C below the first atomic layers,¹³ thereby limiting nucleation and growth of carbide precipitates on the surface. The base pressure of the CIMD chamber is 3×10^{-10} Torr and reaches 2×10^{-9} Torr during deposition. *In situ* 10 keV reflection high energy electron diffraction (RHEED) detects phase transitions at the surface during cleaning and topographical changes during synthesis.

Heteroepitaxial $\text{Si}_{1-x-y}\text{Ge}_x\text{C}_y$ thin films are synthesized on 4 inch Si(100) wafers in a combined ion and molecular beam deposition (CIMD)¹² system. Molecular Si and Ge are evaporated from conventional e-beam sources. A partially ionized (~40%) C⁺ beam is obtained from a solid 99.9995% pyrolytic graphite source. Direct deposition of the ionized C during CIMD, can limit the surface mobility of C by “anchoring” the C below the first atomic layers,¹³ thereby limiting nucleation and growth of carbide precipitates on the surface. The base pressure of the CIMD deposition chamber is 3×10^{-10} Torr and reaches 2×10^{-9} Torr during deposition. *In situ* 10 keV reflection high energy electron diffraction (RHEED) detects phase transitions at the surface during cleaning and topographical changes during synthesis.

Before introduction into the CIMD system, the Si wafers undergo an RCA type cleaning followed by oxide etching and H passivation in a 5:95 HF in methanol solution, and rinsing in methanol. Prior to $\text{Si}_{1-x-y}\text{Ge}_x\text{C}_y$ deposition, H is thermally desorbed and the Si(100) reconstructed to a distinct (2×1) RHEED pattern *in situ* at 560 °C for $t \geq 10$ min.

TABLE I. Film growth conditions and characteristics obtained by RBS and TEM.

Sample	Deposition temperature (°C)	Growth rate (Å/s)	Composition	Thickness (Å)	χ_{\min}
C32	560	0.09	Si _{0.72} Ge _{0.27} C _{0.006}	1000	0.13
C33	560	0.09	Si _{0.71} Ge _{0.28} C _{0.005}	1000	0.12
C34	450	0.07	Si _{0.71} Ge _{0.28} C _{0.005}	800	0.17
C71	450	0.07	Si _{0.72} Ge _{0.28}	1000	0.03

Then a 100 nm Si buffer layer is grown at 560 °C to smoothen the Si surface and to bury C and F residue.¹⁴ The wafer temperature during growth was measured by a thermocouple calibrated by a pyrometer.

The Si and Ge atomic fractions in the films are measured by 2 MeV ⁴He⁺⁺ Rutherford backscattering spectroscopy (RBS). Given the small RBS cross section for C, the low C atomic fraction is detected by nuclear resonance analysis (NRA), using the 4.265 MeV C elastic resonance.¹⁵ The C surface contamination is separated from C in the Si_{1-x-y}Ge_xC_y film by tilting the sample normal 75° with respect to the incident beam and increasing the ⁴He⁺⁺ energy up to 4.31 MeV.¹⁶ Carbon depth profiles are independently verified by secondary ion mass spectrometry (SIMS), using a 25 nA flux of 14.5 keV Cs⁺. Infrared (IR) absorption measurements are performed using a Fourier transform IR (FTIR) spectrometer with a LN₂-cooled HgCdTe detector. A reference spectrum is acquired from a bare Si wafer from the same lot, so that the Si-Si two-phonon mode at 610 cm⁻¹ can be subtracted. Film thickness is characterized both by RBS and cross section transmission electron microscopy (X-TEM). Heteroepitaxial quality is quantified by the minimum yield, χ_{\min} , along the <110> ion channeling axis and by X-TEM.

Table I lists deposition conditions for the heteroepitaxial Si_{1-x-y}Ge_xC_y films, and composition and thickness obtained by RBS and NRA. For comparison, Table I includes a binary Si_{1-x}Ge_x film deposited under similar conditions. The main difference between deposition conditions is the temperature: 560 °C in C32 and C33 and at 450 °C in C34 and C71.

In Fig. 1, SIMS profiles for C32 are shown. Profiles such as the one in Fig. 1 demonstrate that C is uniformly distributed throughout depth.

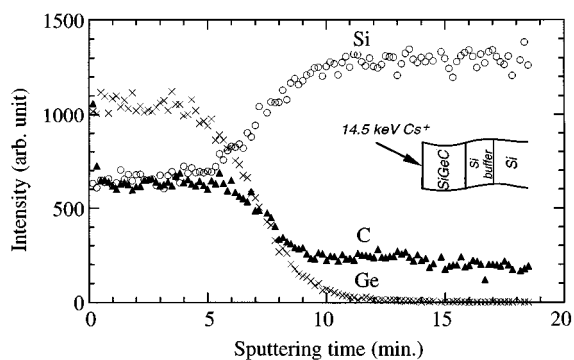


FIG. 1. SIMS profile of C32, showing uniform distribution of all constituents. A sputtering rate of 1.9 Å/s was estimated from the time to the films-substrate cross-over in the SIMS profile and the RBS film thickness.

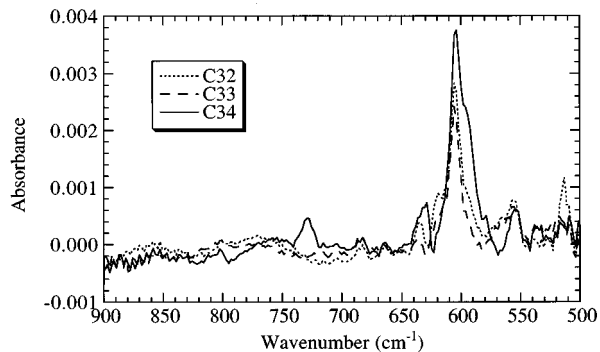


FIG. 2. FTIR spectra of C32 and C33, deposited at 560 °C, and C34 deposited 450 °C. The spectrum for the film grown at 450 °C shows a larger absorption around 607 cm⁻¹ than the films grown at 550 °C indicating more substitutional C. No SiC precipitates are detected at 800 cm⁻¹.

In Fig. 2, IR absorption spectra for C32, C33, and C34 are shown. Substitutional C in Si has a well-established vibrational mode around 605 cm⁻¹, whereas SiC has a vibrational mode around 794–810 cm⁻¹.¹⁷ For C34, deposited at 450 °C, the vibrational mode at 605 cm⁻¹ is observed, but no SiC signal is detected at 800 cm⁻¹. For C32 and C33, deposited at 560 °C, the vibrational mode at 605 cm⁻¹ is much weaker than in C34 but the 800 cm⁻¹ mode is still too weak to be detected. We therefore conclude that the amount of C atoms present at substitutional sites in Si_{1-x-y}Ge_xC_y layers deposited at 450 °C is larger than that deposited at 560 °C. Since there is no indication that C is present as SiC precipitates, it can be assumed that some C in films grown at 560 °C is present either as interstitials or in C-rich clusters.

Figure 3(a) shows a TEM and Fig. 3(c) a HRTEM micrograph of C32, grown at 560 °C. Stacking faults and dis-

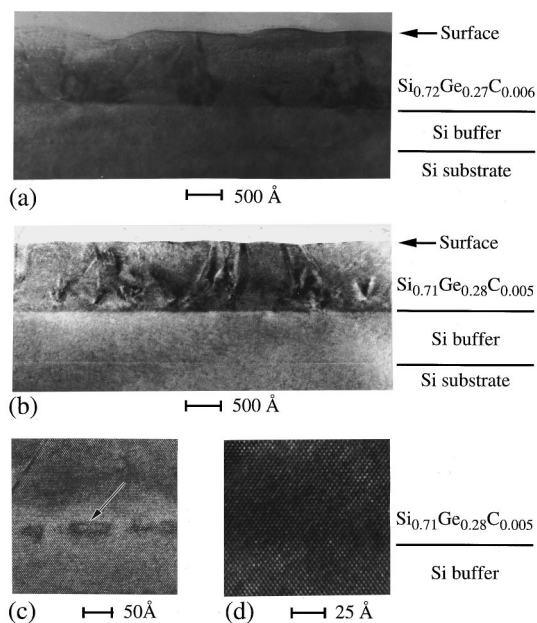


FIG. 3. (a) TEM micrograph of C32 deposited at 560 °C showing a low density of dislocations and stacking faults. (b) TEM of C34, deposited at 450 °C with a similar density of defects as in (a). (c) HRTEM of C32 in a region close to the film/buffer interface, with one of the clusters discussed in the text, marked with an arrow. (d) HRTEM of film/buffer interface in C34 with no observable clusters.

locations are observed, as often seen in relaxed $\text{Si}_{1-x}\text{Ge}_x$ alloys on Si.¹⁸ With a Si:Ge ratio of 7:3, relaxation would be expected also for a binary $\text{Si}_{1-x}\text{Ge}_x$ film of 1000 Å thickness.¹¹ Moreover, spherical clusters of 20–50 Å size, which are coherent with the matrix and separated by roughly 50 Å, are observed. These clusters exhibit bright contrast in the bright field image, indicating a region with lower average atomic Z . The clusters line-up parallel to the (100) interface. Close to the film surface these clusters have similar shape and size. Closer to the film/buffer interface some clusters have grown in a direction parallel to the interface at the expense of the size of other clusters. These clusters have been exposed to the growth temperature for a longer time than clusters closer to the surface, thus indicating a ripening process, caused by thermal diffusion. Preliminary energy dispersive x-ray analysis, with a 100 Å diameter electron beam, shows that the clusters are Ge deficient.¹⁴ In dark field TEM, the clusters observed in films grown at 560 °C also exhibit contrast,¹⁴ indicating that even though there are no extended defects associated with the clusters, the lattice in the clusters is distorted.

Figure 3(b) shows a TEM and Fig. 3(d) a HRTEM micrograph from C34, deposited at 450 °C. A similar density of stacking faults as in C32 and C33 is observed, but no small clusters.

To estimate C diffusion in $\text{Si}_{1-x-y}\text{Ge}_x\text{C}_y$ during growth, we determine the C diffusion length from, $x = (4Dt)^{1/2}$, where x is the diffusion length, t is the diffusion time, and D is the diffusivity. Assuming the diffusivity of C to be similar to that in Si we used⁹ $D = 1.9 \exp(-3.1 \pm 0.2/kT)$ cm²/sec, where k is the Boltzman constant in eV/K, and T is the temperature. For 2 h diffusion the C diffusion length would thus be $2.4 \text{ \AA} \leq x \leq 40 \text{ \AA}$ at 560 °C and $0.074 \text{ \AA} \leq x \leq 1.8 \text{ \AA}$ at 450 °C. This indicates that C bulk diffusion may be fast enough to explain the secondary phase clusters with low average atomic Z , seen in $\text{Si}_{1-x-y}\text{Ge}_x\text{C}_y$ films grown at 560 °C, whereas C bulk diffusion at 450 °C is too slow to cause any clustering, in agreement with our observations. Since there is no indication of SiC formation in the FTIR spectra (Fig. 2), we propose that the clusters may be C rich, secondary phase, precursors to SiC precipitates, similar to a Guinier-Preston formation. A C-rich secondary phase precursor to SiC precipitates has been proposed previously for C in Si.¹⁰

The higher χ_{\min} of $\text{Si}_{1-x-y}\text{Ge}_x\text{C}_y$ film deposited at 450 °C compared to the films at 560 °C (Table I), may at first seem contradictory to the observed temperature dependence of the C substitutionality. Furthermore, strain measurements performed on these films by doing RBS angular scans across a (111) axis shows that $\text{Si}_{1-x-y}\text{Ge}_x\text{C}_y$ films grown at 450 °C have lower strain than do films grown at 560 °C.¹⁹ However, when C is incorporated at substitutional sites in heteroepitaxial $\text{Si}_{1-x-y}\text{Ge}_x\text{C}_y$ on Si(100), there may be a distribution of different bond lengths,^{20,21} while the average lattice constant follows Vegard's law. This would increase χ_{\min} compared to a perfect cubic lattice. The difference in χ_{\min} between $\text{Si}_{1-x-y}\text{Ge}_x\text{C}_y$ films and $\text{Si}_{1-x}\text{Ge}_x$ films (Table I), which is larger than would be expected from TEM, supports this notion. At a growth temperature of 560 °C, C is partly incorporated into the C-rich clusters, which supposedly have

a smaller lattice parameter and thus allow the remaining C deficient regions to relax somewhat. The C deficient regions are expected to be more $\text{Si}_{1-x}\text{Ge}_x$ -like and have less bond length distribution than films where C is mainly substitutional. This could lead to a lower overall χ_{\min} . That relaxation by cluster formation is slightly less effective in reducing strain is reasonable but difficult to quantify.

In summary, by comparing characterization by TEM, FTIR, and ion channeling, it has been shown that the growth temperature versus time window must be chosen carefully to inhibit not only SiC precipitation but also the formation of Ge-deficient clusters, tentatively identified as C-rich. It is that it is not possible to directly detect these clusters by IR spectroscopy and, since they basically probe the same physical quantity, probably not by Raman spectroscopy either. Experiments with C concentrations up to 9% have been conducted and are reported elsewhere.²²

This work was supported AFSOR/ARPA under Contract No. F49620-43-C-0018, by SEMATECH under Contract No. 74086276 and by NSF under Contract No. DMR-93-14326 (the HTRTEM facility). H. J. gratefully acknowledge post-doctoral support from Wenner-Gren Center Foundation. H. Werthén Foundation, Ph.D. M. Wallenberg Foundation for Education in International Industrial Enterprise, and P. E. Lindahl Foundation. 4 in. Si wafers were donated by Motorola Inc. via Fritz Wilson and Ronald Swift.

- ¹J. C. Bean, *Science* **230**, 127 (1985).
- ²C. A. King, J. L. Hoyt, and J. F. Gibbons, *IEEE Trans. Electron Devices* **36**, 2093 (1989).
- ³R. A. Soref, *J. Appl. Phys.* **70**, 2470 (1991).
- ⁴K. Eberl, S. S. Iyer, S. Zollner, J. C. Tsang, and F. K. LeGoues, *Appl. Phys. Lett.* **60**, 3033 (1992).
- ⁵T. Nozaki, Y. Tatsurugi, and N. Akiyama, *J. Electrochem. Soc.* **117**, 1566 (1970).
- ⁶R. W. Olesinski and G. J. Abbaschian, *Bull. Alloy Phase Diagrams* **5**, 484 (1984).
- ⁷J. W. Strane, H. J. Stein, S. R. Lee, B. L. Doyle, S. T. Picraux, and J. W. Mayer, *Appl. Phys. Lett.* **63**, 2786 (1993).
- ⁸H. C. Abbink, R. M. Broudy, and G. P. McCarthy, *J. Appl. Phys.* **39**, 4673 (1968).
- ⁹R. C. Newman and J. Wakefield, *Metallurgy of Semiconductor Materials*, edited by J. B. Schroeder (Interscience, New York, 1962), Vol. 15, p. 201.
- ¹⁰J. W. Strane, H. J. Stein, S. R. Lee, S. T. Picraux, J. K. Watanabe, and J. W. Mayer, *J. Appl. Phys.* **76**, 3656 (1994).
- ¹¹K. Eberl, S. S. Iyer, J. C. Tsang, M. S. Goorsky, and F. K. LeGoues, *J. Vac. Sci. Technol. B* **10**, 934 (1992).
- ¹²N. Herbots and O. C. Hellman, US Patent #4,800,100 (1989).
- ¹³N. Herbots, O. C. Hellman, and O. Vancauwenberghe, *Mater. Res. Soc. Symp. Proc.* **235**, 749 (1992).
- ¹⁴P. Ye, Ph.D. Thesis, Arizona State University (1995).
- ¹⁵J. A. Leavitt, L. C. McIntyre Jr., P. Stoss, J. G. Oder, M. D. Ashbaugh, B. Dezfouly-Arjomandy, Z.-M. Yang, and Z. Lin, *Nucl. Instrum. Methods B* **40/41**, 776 (1989).
- ¹⁶S. Hearne, N. Herbots, J. Xiang, P. Ye, and H. Jacobsson, *Nucl. Instrum. Methods B* (to be published).
- ¹⁷A. R. Bean and R. C. Newman, *J. Phys. Chem. Solids* **32**, 1211 (1971).
- ¹⁸F. M. Ross, R. Hull, D. Bahnick, J. C. Bean, L. J. Peticolas, R. A. Hamm, and H. A. Huggins, *J. Vac. Sci. Technol. B* **10**, 2008 (1992).
- ¹⁹S. Segó, R. J. Culbertson, D. J. Smith, Z. Atzmon, and A. E. Bair, *J. Vac. Sci. Technol. A* (to be published).
- ²⁰B. Dietrich, H. J. Osten, H. Rücker, M. Methfessel, and P. Zaumseil, *Phys. Rev. B* **49**, 17185 (1994).
- ²¹J. Menéndez, P. Gopalan, G. S. Spencer, N. Cave, and J. W. Strane, *Appl. Phys. Lett.* **66**, 1160 (1995).
- ²²H. Jacobsson, P. Ye, N. Herbots, S. Hearne, and J. Xiang, *Nucl. Instrum. Methods. B* (to be published).